SAFETY FLIGHT TESTING FOR CARGO UAV DEVELOPMENT

Kakuya Iwata*[1], Keisuke Yamada*[2], Ryuzo Horiuchi*[2], Akiya Kamimura*[1]
***[1]Intelligent System Research Institute,**
***[2]Research Institute for Measurement and Analytical Instrumentation,**
National Institute of Advanced Industrial Science and Technology (AIST), Tsukuba, Japan
Keywords: *UAV, CargoUAV, UAV safety mechanism*

Abstract

Recently, Requirement of capability to autonomous fling machine is expanded by brand-new application of UAV. Many kinds of application as inspection, surveillance, aerial photo, aerial video shooting, aerial cargo transportation, OPV(optionally piloted vehicle) require new kinds of safety technologies such as precision location control, self-health monitoring, autonomous emergency avoidance and so on. Technologies of small reliable turbine propulsion, crushable safety, safety take-off test system and safety responsibility aggregation system are part of such safety technologies and they are one of the solutions of flight reliability and crash safety requirements. In this paper, we report the progress of our technology development to improve the safety of these unmanned aerial vehicles and its system.

1. Introduction

It has been opened commercial use of Unmanned Aerial Vehicle (UAV) by quite small size UAV called "Drone" from around 2010. Now the drone which flights instead of human eyes becomes smaller, the drone which works like human hands is getting larger. National Institute of Advanced Industrial Science and Technology (AIST) had been working on research and development of transportation for the unmanned aircraft since 2004 (Cargo UAV). [1-5] It has developed a pendulum stability control type fixed wing unmanned aircraft flying at 100km/h in total weight 150kg and wingspan 10m as shown in Fig.1. [4] The problem of such a large UAV development is how to keep safety during research and development. In this paper, elements of solutions for safety UAV development are reported.

Fig.1 Cargo UAV prototype in AIST

2. Safety turbine propulsion for UAV

Turbine propulsion machines are considered to be one of the propulsion machines for enhancing safety.

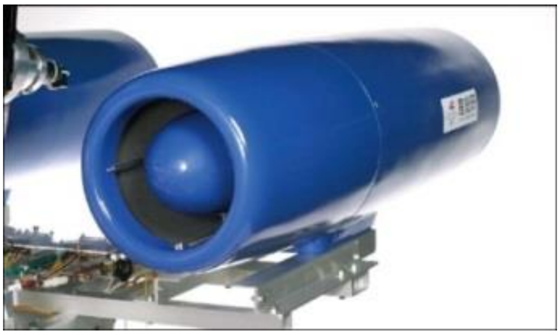

Fig.2 Low noise turbo jet propulsion for UAV

This is because the turbojet engine has no dangerous exposed large rotation structure, no engine stop, no large vibration and no low reliability. We have developed a small jet engine for UAV with low noise capability as shown in Fig.2.

The jet engine for UAV has a thrust of 20 kg, weight is 8 kg, length is 1 m, and diameter is 32 cm. The maximum number of revolutions is 90,000 rpm. Figure 3 indicates the noise absorption structure of the UAV jet engine. [3]

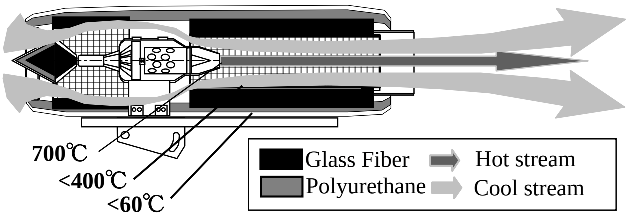

Fig.3 Noise absorption material cooling system

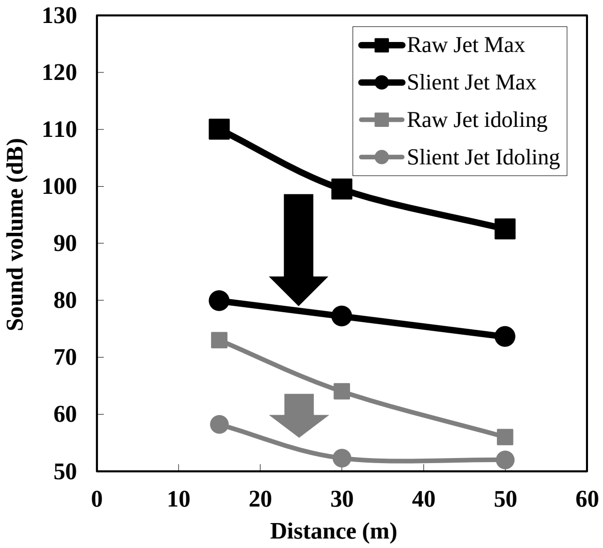

Fig.4 Noise reduction of silent jet

There are two kinds of noise absorption material in the noise reduction structure and bypass air cooling keeps the temperature gradient as shown in Fig.3. Figure 4 indicates the results of field measurement of noise reduction effect. These are measured by A-weighted sound pressure level at the back (exhaust) side of jet engine. At the maximum thrust power, extremely large noise reduction of 30 dB is measured.

The field measurement of jet engine requires lots of attention about the large thrust force, hot exhaust stream of 700 degree C, weather condition, safety environments and large noise.

So, we attempt to use reverberation chamber method using sound generator as shown in Fig.5 in order to obtain high performance development and evaluation method for safety, speed and cost.

Fig.5 Noise reduction measurement system in reverberation chamber

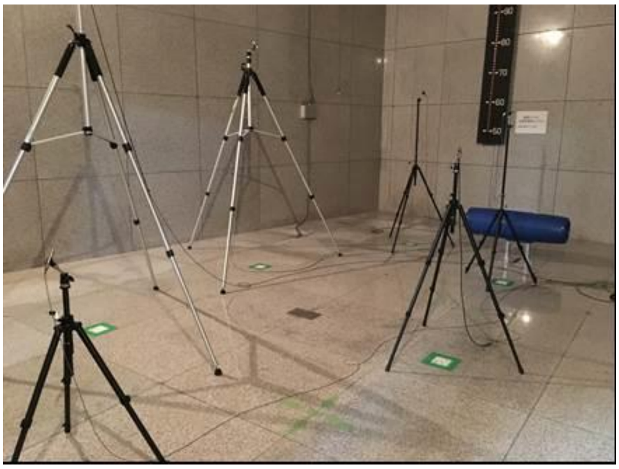

Fig.6 Location and formation of sound detectors

Figure 6 shows the location and formation of the sound detectors (microphones), and also the location of sound generator built in the silencer unit of the silent jet engine.

The result of noise reduction effect measured by reverberation chamber method is indicated in Fig.7. The reduced sound power level is the value with the silencer minus the value without the silencer.

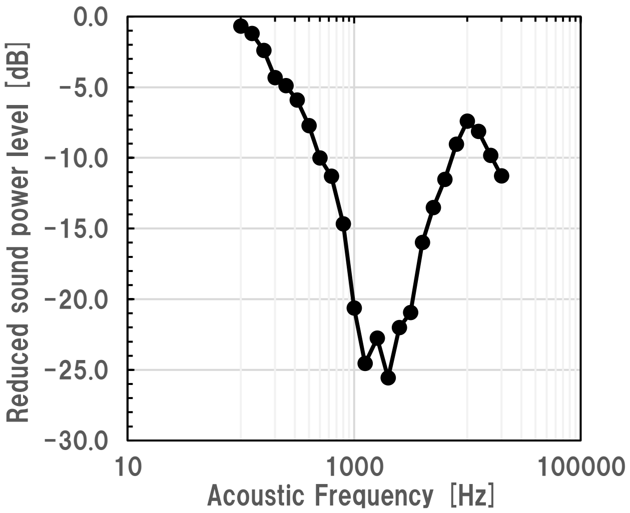

Fig.7 Reduced sound power level measured by reverberation chamber method

Large noise reduction effect of 26 dB is observed around 2000Hz as shown in Fig.7. This value is almost comparable to the 30dB in Fig.4 taking account of the difference of the method of measurement, environment, atmospheric flow, sound source and so on.

So, it is successfully obtained safety evaluation method for noise reduction system of turbojet engine for UAV.

3. Crushable safety technology of UAV

The capabilities of crushable safety are necessary for large UAVs. The vertical frame at the red circle in Fig. 8 is the crushable safety frame of Cargo UAV.

Fig.8 Crushable safety structure in Cargo UAV

This vertical frame absorbs the impact force when this cargo UAV crushes. In order to create and design this crushable safety structure of Cargo UAV, strength analysis is essential. The strength of this cargo UAV crushable vertical frame is determined by simulation and experimental measurement.

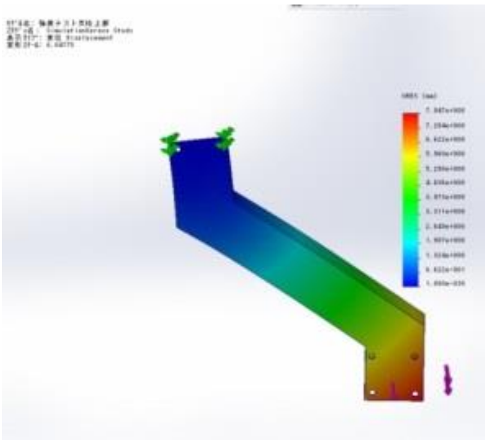

Fig.9 Strength analysis of the crushable frame

Fig.10 Strength test of the crushable frame

Figure 9 indicates the results of the strength simulation analysis and Fig.10 shows the strength test in the case of compressive deformation of the cargo UAV crushable safety structure. We decided the airworthiness of this cargo UAV from +4G to -2G according to the regulation of Deutscher Hängegleiterverband e.V.(DHV). As a result of the strength measurement, it was found that elastic deformation occurs up to + 4 G and plastic deformation occurs from + 4 G to + 6 G. This + 6 G is + 4 G multiplied by safety factor 1.5. The simulation using the physical property values of aluminum alloy is able to calculate the value very close to the actual measurement value.

In order to obtain crushable safety capability, strength analysis as shown in Fig.11 should be done for large multi-rotor type UAV as shown in Fig.12. In the simulation using the carbon fiber composite material, the uniformity of the physical property values of the carbon fiber composite material is low, so that a deviation occurs from the measured value of the strength test.

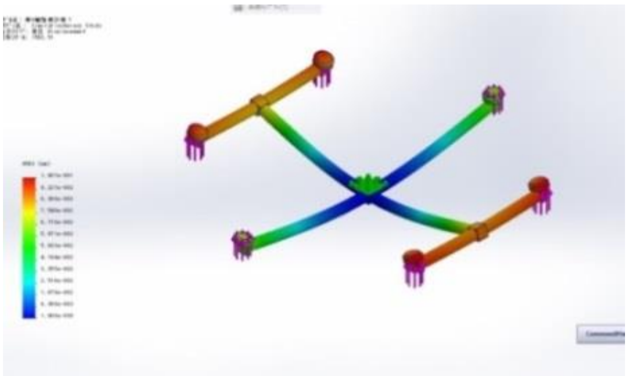

Fig.11 The frame structure strength analysis

Fig.12 Large multi-rotor cargo UAV

4. Safety flight test method

A large multi-rotor UAV is also used at the time of infrastructure inspection. The UAV in Fig. 13 was developed to perform a hammering test.

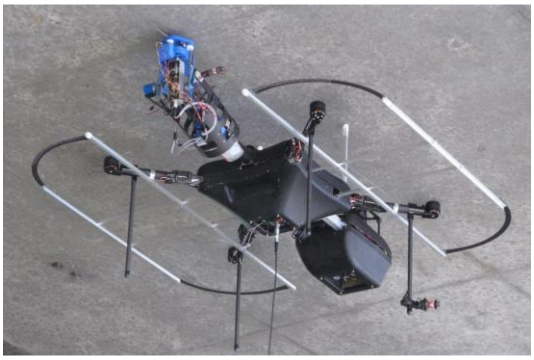

Fig.13 Hammering UAV [6]

It is indispensable to use safety UAV net in Fig.14 due to avoid accident during the development of inspection process.

Fig.14 Safety UAV net

For the case of Cargo UAV flight test, we developed the safety guide wire system.

Roll axis attitude controlling procedure is shown in Fig.15. Motion equations of roll movement are following;

$$[M_1 l_1^2+(1/12)M_2(l_2^2+a^2)]d\theta_1^2/dt+ (1/4)C_D S\rho\theta_1^2 cos(d\theta_1 /dt)- M_1 g sin\theta_1 = T_z \quad (1)$$

$$M_1 l_1^2\theta_2+(1/12)M_2(l_2^2+a^2)d\theta_1^2/dt+ (1/4)C_D S\rho\theta_1^2 cos(d\theta_1/dt)- M_1 g sin(\theta_1 +\theta_2) = nK_f I \quad (2)$$

where, CCW is positive, I is motor current [A], a is wing thickness [m], g is gravity acceleration [m/s^2], M_1 is mass of the body [kg], M_2 is mass of the wing [kg], J_1 is moment of inertia of the body [kgm^2], J_2 is moment of inertia of the wing [kgm^2], L_1 is length of between the body and wing [m], L_2 is half length if the wing span [m], K_f is torque constant of the motor [Nm/A], n is reduction ratio of the gear, ρ is density of standard atmosphere [kg/m^3], C_D is drag coefficient [m/s^2], S is area of the wing [m^2] and T_z is disturbance.[4]

The flying robot of Cargo UAV prototype performed jump flight test using the Safety guide wire as shown in Fig. 16.

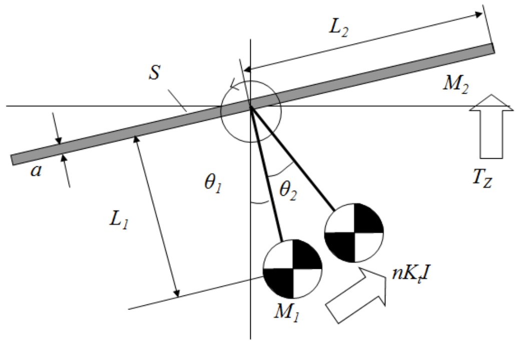

Fig.15 Roll axis attitude control procedure

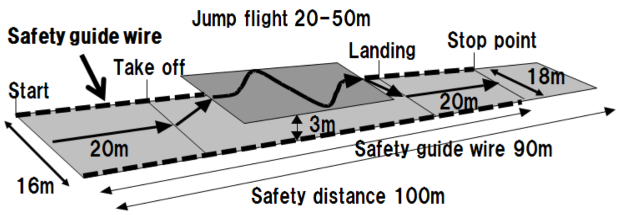

Fig.16 Test flight with safety guide wire

Flight test using safety guide wire was done to observe the attitude stabilizing effect in a state that does not actually controlled by attitude sensor feedback. In order to increase the take-off speed at an early stage, it utilizes a towing as shown in Fig. 17.

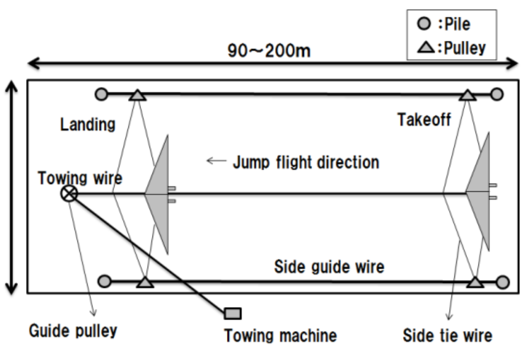

Fig.17 Safety test method using guidewire (top view)

At the time of take-off, the cargo UAV accelerated by the thrust of the jet engine and towing of the wire. Fig. 18 shows a view from the side of safety jump flight test method according to the guide wire and towing. The towing wire and side wires are connected on the machine body. Two pulleys of right and left side travel on the two wires on the ground.

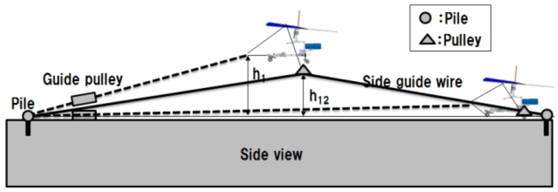

Fig.18 The towing method according to the safety test (as viewed from the side)

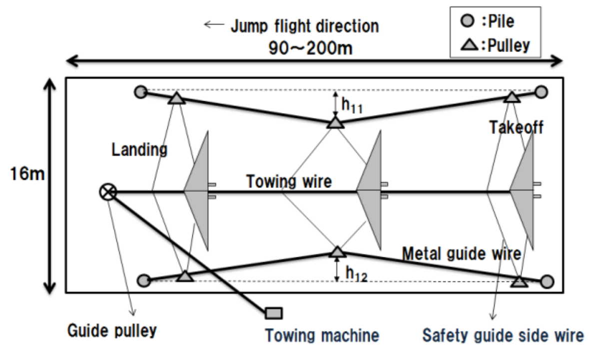

Fig.19 Elastic deformation of two side wires

The wing of the cargo UAV is fixed to a pulley on the left and right of the wire, and it is never out of the stable orbit of guide wires. Two guide wires lift together with the flight of the cargo UAV and deform by the tension.

The elastic deformation of the side wires is illustrated in Fig. 19. Two right and left of the guide wire plays the role of a spring as shown in Fig. 20.

Figure 20 shows the mechanics of the Safety guide wire flight test method.

The f_1 and f_2 are tension of left and right wing, and the elastic deformation length of the side wire indicates as h_{11} and h_{12}, and holds the following equation of motion.

$$(M_1+M_2)d^2h/dt = f_1+f_2 \quad (3)$$

$$J_2d^2\theta_1/dt = -L_2f_1+L_2f_2 \quad (4)$$

$$r_1 = (1/2)\rho C_dS(d^2h_{11}/dt) \quad (5)$$

$$r_2 = (1/2)\rho C_dS(d^2h_{12}/dt) \quad (6)$$

$$f_1 = k_1h_{11}+(1/2)\rho C_dSd^2h_1/dt \quad (7)$$

$$f_2 = k_2h_{12}+(1/2)\rho C_dSd^2h_1/dt \quad (8)$$

$$h_{11} = h_1/\sin\theta_{s1} \quad (9)$$

$$h_{12} = h_1/\sin\theta_{s2} \quad (10)$$

Here, C_d indicates the damping coefficient due to air drag of the wing. Moreover, m_{11} and m_{12} indicates the weight of the two side wires. Distance of the guide wire becomes longer, and m_{11} and m_{12} increases and k_1 and k_2 are not constant in this case.

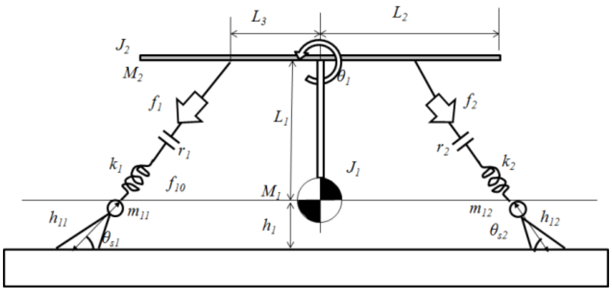

Fig.20 Safety guide wire flight test method

Fig.21 shows the state of the model of the roll axis attitude control
According to Fig. 21, following equations are obtained.

$$nK_fI + (f_2-f_1) = T_z \qquad (11)$$

In this experiment, it revealed that f_1 and f_2 were larger than the disturbance T_z. So, it was possible to ensure a stable posture. Further, by measuring the f_1 and f_2 and θ_1, the control amount required was shown to be derived.

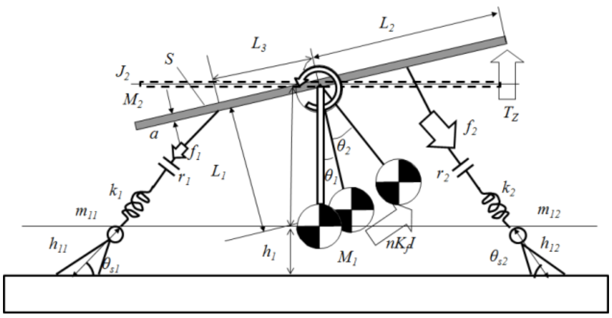

Fig.21 Attitude control of safety guide wire method

The attack angle of the wing is measured by the angle of the keel.
When the attack angle was set to 23 degrees, Cargo UAV prototype successfully take off for the first time. Thereafter, experiments were conducted by varying the attack angle from 25 to 27 degrees. Since the stall at the wing tip was occured in 28.5 degrees, it was confirmed that there is an optimum point of maximum angle of attack to 27 degrees. Then, it was implemented the observation of the minimum angle of attack. As a result, it was observed optimum point of minimum attack angle of 20 degrees. It shows the state of the flight test at the optimum angle of attack 27 degrees in Fig. 22.


Fig.22 The flight experiment of the cargo UAV

Figure 23 shows the measured elastic force of side wires. The difference of wire tension between right and left shows the location and attitude of the cargo UAV prototype. The cargo UAV starts from the runway point of 0m, takes off at 20m, takes landing at 180m and stops at 195m.
Figure 24 shows that the attitude of the cargo UAV was tilted due to the difference in tension on the left and right. The difference of the tension generates due to the difference of spring constants k_1 in (7) and k_2 in (8).

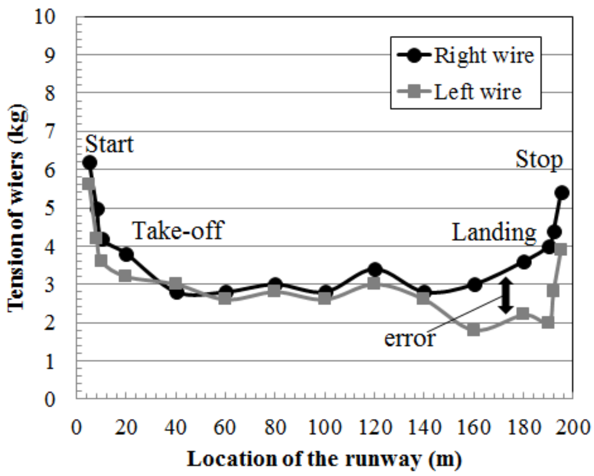

Fig.23 Measured tension difference between right and left wires

These spring constants are able to adjust by controlling the tension of the left and right wires. So, it is important to adjust to $k_1 = k_2$ in this safety guide wire method.

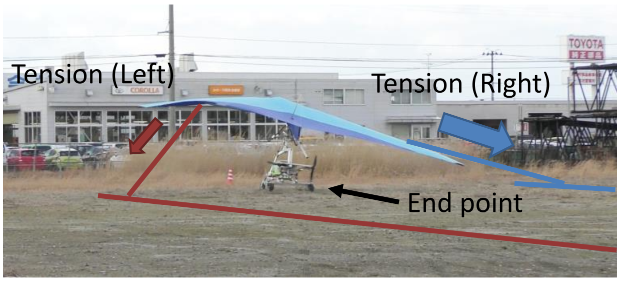

Fig.24 Tension difference between right and left wire at the end runway point of 195m

5. Safety responsibility aggregation system

For the future, Service provider is necessary to create the safety business model of cargo UAV transportation industry as shown in Fig.25. The service provider will manage segregated UAV highway using UTM. The virtual air way network creation by the service provider will also create a market of safety autonomous aerial transportation, and the market will make the service provider larger. Such a spiral up of the industry is expected.

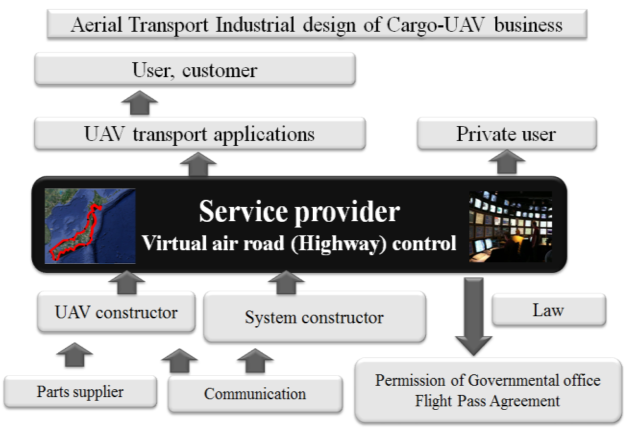

Fig.25 Required Service Provider for Cargo UAV transportation industry.

6. Summary

We compiled the safety technologies which we developed in this paper. These safety technologies will contribute to improving the efficiency of brand-new large UAV development. The cargo UAV technology for aerial unmanned transportation is still under development. The method of safety and efficient development is important. The guide wire test flight method that reported in this paper is one of the efficient methods for safety development of cargo UAV. At present, this safety guide test flight method is used in Niigata Sky project. It has implemented the development and unmanned aircraft development of unmanned aircraft for small silent jet engine to contribute to the sprouting of the unmanned aircraft industry. Activities by these local municipalities created a new regional brand, leading to activation of the region. For these regional cargo UAV development activities, it is important to carry out numbers of examinations with safe. This safety guide wire test method as flight test technique is shown to be effective to obtain safety examination environment.

For the future, Service provider is necessary to create the business model of aerial unmanned transportation industry as shown in Fig.25. The service provider is a pioneer of the UAV highway as shown in Fig.26.

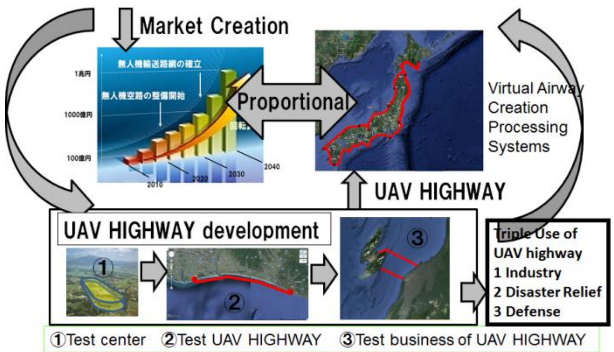

Fig.26 Spiral up between UAV highway creation and market creation.

The virtual air way creation by service provider will create a market of autonomous aerial transportation and the market will make the service provider large. Such a spiral up construction of the cargo UAV industry is expected.

Acknowledgements

AIST conducts the NIIGATA SKY PROJECT (NSP) consisting of jet engine and cargo UAV development. The authors would like to thank the members of NIIGATA SKY PROJECT. The hammering UAV development is based on results obtained from a project commissioned by the New Energy and Industrial Technology Development Organization (NEDO).

References

[1] K.Iwata, M.Onda, M.Sano, K.Komoriya, "UAV for Small Cargo Transportation", AIAA Infotech Aerospace 2007 Conference, AIAA Meeting Papers On DISC No.9, AIAA2007-2784.

[2] K.Iwata, N.Hashimoto, K.Komoriya, "Aerial Robotic System for Transportation and Logistics", Journal of Mechanical Systems for Transportaion and Logistics (JMTL), Vol.1, No.1, pp.146 -157, 2008.

[3] K.Iwata, K.Matsubara, K.Kawasaki, K.Abe, H. Koshikizawa and O.Matsumoto, "Turbojet Engine for Cargo UAV (ACR)", Journal of Robotics and Mechatronics, Vol.24 No. 6, December 20, 2012.

[4] K.Iwata and O.Matsumoto, "Research of Cargo UAV for Civil Transportation", Journal of Unmanned System Technology, Vol.1, No.3, pp.89-93, (2013)

[5] K.Iwata and O.Matsumoto, "Cargo UAV (Cargo UAV)", Journal of Robotics and Mechatronics, Vol.26, No.3, p.394, (2014)

[6] https://wisdom.nec.com/en/solutions/2017033102/02.html